ACS APPLIED MATERIALS & INTERFACES

Research Article

www.acsami.org

Gellan Gum-Hyaluronic Acid Spongy-like Hydrogels and Cells from Adipose Tissue Synergize Promoting Neoskin Vascularization

Mariana Teixeira Cerqueira,[†,‡] Lucília Pereira da Silva,[†,‡] Tírcia Carlos Santos,[†,‡] Rogério Pedro Pirraco,[†,‡] Vítor Manuel Correlo,[†,‡] Rui Luís Reis,[†,‡] and Alexandra Pinto Marques*[,†,‡]

[†]3B's Research Group - Biomaterials, Biodegradables and Biomimetics, University of Minho, Headquarters of the European Institute of Excellence on Tissue Engineering and Regenerative Medicine, AvePark4806-909, Taipas, Guimarães, Portugal

[‡]ICVS/3B's, PT Government Associate Laboratory, Braga/Guimarães, Portugal

ABSTRACT: Currently available substitutes for skin wound healing often result in the formation of nonfunctional neotissue. Thus, urgent care is still needed to promote an effective and complete regeneration. To meet this need, we proposed the assembling of a construct that takes advantage of cell-adhesive gellan gum-hyaluronic acid (GG-HA) spongy-like hydrogels and a powerful cell-machinery obtained from adipose tissue, human adipose stem cells (hASCs), and microvascular endothelial cells (hAMECs). In addition to a cell-adhesive character, GG-HA spongy-like hydrogels overpass limitations of traditional hydrogels, such as reduced physical stability and limited manipulation, due to improved microstructural arrangement characterized by pore wall thickening and increased mean pore size. The proposed constructs combining cellular mediators of the healing process within the spongy-like hydrogels that intend to recapitulate skin matrix aim to promote neoskin vascularization. Stable and *off-the-shelf* dried GG-HA polymeric networks, rapidly rehydrated at the time of cell seeding then depicting features of both sponges and hydrogels, enabled the natural cell entrapment/encapsulation and attachment supported by cell-polymer interactions. Upon transplantation into mice full-thickness excisional wounds, GG-HA spongy-like hydrogels absorbed the early inflammatory cell infiltrate and led to the formation of a dense granulation tissue. Consequently, spongy-like hydrogel degradation was observed, and progressive wound closure, re-epithelialization, and matrix remodelling was improved in relation to the control condition. More importantly, GG-HA spongy-like hydrogels promoted a superior neovascularization, which was enhanced in the presence of human hAMECs, also found in the formed neovessels. These observations highlight the successful integration of a valuable matrix and prevascularization cues to target angiogenesis/neovascularization in skin full-thickness excisional wounds.

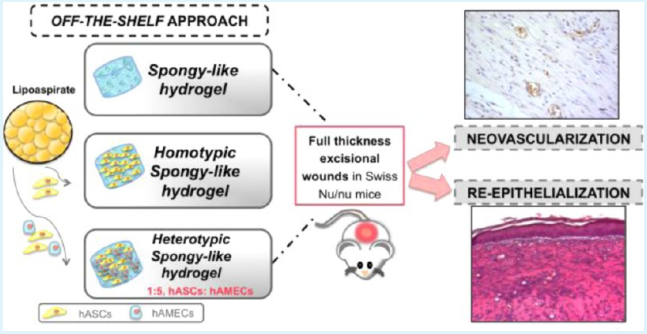

KEYWORDS: *skin, tissue engineering, gellan gum, hyaluronic acid, vascularization, stem cells*

INTRODUCTION

The healing of deep skin wounds in adults takes place by both undesirable wound contraction and scar formation, leading to nonfunctional neotissue formation.[1] To tackle this problem, varied skin tissue engineered substitutes based on polymeric matrices derived from both natural (collagen,[2,3] hyaluronic acid (HA),[4] gelatin,[5] fibrin,[6] laminin, and elastin[7]) and synthetic (polypropylene,[8] polycaprolactone,[9] and polyethylene terephthalate[10]) sources have been proposed.

Emphasis has been given to scaffolding matrices that are thought to reduce/avoid skin contraction during the regeneration process. The mimicking of tissue extracellular matrix (ECM) has been seen as a route to be pursued. The use of hydrogels that are extremely hygroscopic[11] and potentially depicting soft tissue-like mechanical properties[3] for wound healing purposes has been explored. However, hydrogels, except for those that are protein-derived[3,12] or are combined/modified with these or with specific cell-adhesive peptide sequences,[13−17] act as mere cell delivery vehicles. While contributing to improved cell engraftment,[18] they still fail at providing biological cues due to the lack of cell adhesion sites in their networks.[19] This might be particularly relevant to achieve an appropriate revascularization of the skin tissue substitutes that so far does not occur in a favorable time fashion and that has been hampering their success.[20,21] Different approaches have been followed to improve wound healing by promoting a faster and better vascularization of the skin substitutes.[22−30] The incorporation of soluble angiogenic factors, such as vascular endothelial growth factor[25] or basic fibroblast growth factor,[26] the genetic modification of the transplanted cells to produce angiogenic proteins,[27,28] as well as the prevascularization of matrices and scaffolds with progenitor or endothelial cells,[29−31] are the most explored. Prevascularization turned out to be the most efficient in promoting inosculation and

Received: July 10, 2014
Accepted: October 31, 2014
Published: October 31, 2014

consequently in achieving a superior outcome. Despite the significant range of progenitor and endothelial cells that have been used in experiments, along with a wide assortment of scaffolds, these strategies still fail in the recapitulation of the *in vivo* process. In fact, one of the causes of this problematic seems to be the source of endothelial cells; endothelial progenitor cells,[31] umbilical vein endothelial cells,[32] or microvascular endothelial cells[29] are usually from allogeneic sources and if autologous, have limited availability and thus relevance in a clinical setting.

Mesenchymal stem cells (MSCs), including adipose stem cells (ASCs), have been known to release paracrine factors and thus influence different host cells during wound healing. Wound closure acceleration, improved neovascularization, and reduced scar formation have been associated in particular to ASCs,[33−36] which, in addition to their immunomodulatory properties, represent valuable features from a cell therapy perspective.[37] In one of our previous works, we were also able to demonstrate that hASCs embedded in their own ECM as cell sheets contributed to neoepidermal morphogenesis but in a way that was dependent on the nature of the ECM,[38] confirming the importance of the matrix in which cells are embedded. We have previously reported the development of cell-adhesive gellan gum (GG)-based matrices with physical properties between sponges and hydrogels[39,40] that, although not capable of sustained self-organization of the freshly isolated skin cellular fractions, impacted early vascularization in full-thickness mice wound healing. These results suggested that GG-hyaluronic acid (HA) spongy-like hydrogels provided a suitable environment to sustain endothelial cell survival and phenotype/functionality.[41] Thus, considering that by providing cells with a valuable matrix that would permit their natural organization and interaction prior to implantation would be beneficial, we propose a tissue-engineered construct combining a GG-HA spongy-like hydrogel and adipose tissue microvascular endothelial cells and stem cells aiming to promote skin wound neovascularization. The proposed approach takes advantage of the angiogenic elements that can be isolated from a single cell source, adipose tissue, and an *off-the-shelf* three-dimensional (3D) structure that mimics skin ECM composition and, upon hydration, presents similarities with its physical properties.

MATERIALS AND METHODS

1. Gellan Gum-Hyaluronic Acid Spongy-like Hydrogels. *1.1. Preparation.* GG-HA spongy-like hydrogels were prepared as previously described.[39,40] Briefly, a solution of 0.75% (m/V) hyaluronate (1.5 MDa, LifeCore Biomedical, U.S.) and 1.25% (m/V) gelzan (Sigma-Aldrich, France) was prepared at 90 °C and then transferred onto 24-well plates. The addition of divalent cations was performed to form the hydrogels by ionic cross-linking. Phosphate-buffered saline (PBS, Sigma, U.S.) solution was added to the hydrogels for further hydration for 48 h. Following that, hydrogels were frozen at −80 °C overnight and then freeze-dried (Telstar, Spain) for 3 d by hydration with culture medium at the time of cell seeding. Dried polymeric networks and spongy-like hydrogels were photographed using a Stereo Microscope Stemi 1000 (Zeiss, Germany).

1.2. Microcomputed Tomography (micro-CT). Dried polymeric networks microarchitecture was analyzed using an X-ray Microtomography System Skyscan 1072 scanner (Skyscan, Belgium) in a high-resolution mode with a pixel size of 11.3 μm and integration time of 1.7 s. The X-ray source was used at 35 keV energy and 215 μA current. A binary picture was obtained through the transformation of representative data sets of 250 slices, using a dynamic threshold of 60e255 (gray values) to distinguish polymer material from pore voids.

1.3. Scanning Electron Microscopy (SEM). Gold-coated (Cressington Sputter Coater, U.K.) GG-HA dried polymeric networks were analyzed by SEM using XL 30 ESEM-FEG microscope (Phillips, U.K.) at an accelerating voltage of 15 kV.

1.3.1. Cryo-SEM. A JEOL JSM 6301F/Oxford INCA Energy 350/Gatan Alto 2500 microscope (JEOL, Japan) was used to analyze the microstructure of spongy-like hydrogels and the hASCs organization within GG-HA spongy-like hydrogels. Samples were positioned on a vacuum transfer rod, slam-frozen to −210 °C in N_2 slush, and moved to the cryostat chamber at −130 °C. The top rivet was flicked off to produce a fractured surface that was sublimed at −90 °C for 2 min and coated with gold/palladium.

1.4. Water Uptake. Water uptake measurements were carried out by immersing dried polymeric networks in α-MEM culture medium up to 7 d at 37 °C. Samples were weighted initially (Wd) and then again 1, 3, 6, 9, 24, 48, 72, 96, 108, and 156 h postimmersion in culture medium, as spongy-like hydrogels, and after removal superficial liquid (Ww). Percentage of water uptake was obtained using the following equation:

$$\text{Wateruptake}(\%) = (\text{Ww} - \text{Wd})/\text{Wd} \times 100.$$

where Wd = weight of dried polymeric networks and Ww = weight of spongy-like hydrogels.

2. Cell Isolation. hASCs and hAMECs were both isolated from human subcutaneous adipose tissue obtained from liposuction procedures (three different donors). Tissue samples were provided by Hospital da Prelada (Porto), after patient's informed consent and 3B's Research Group/Hospital ethical committees approval. After digestion with 0.05% Collagenase type II (Sigma, U.S.), a filtration and centrifugation at 800 *g* were performed, and the stromal vascular fraction (SVF) was obtained. The SVF pellet was incubated with red blood cell lysis buffer (155 mM of ammonium chloride, 12 mM of potassium bicarbonate and 0.1 M of ethylenediaminetetraacetic acid (all from Sigma-Aldrich, Germany) in distilled water) for 10 min at room temperature and further centrifuged at 300 *g* for 5 min. The red blood cells-free SFV was either resuspended in α-MEM medium (Invitrogen, U.S.) containing 10% fetal bovine serum (FBS) (Invitrogen, U.S.) and 1% antibiotic/antimycotic (Invitrogen, U.S.), or in endothelial growth medium (EGM-2MV) (Lonza, U.S.), respectively, for hASCS and hAMECs isolation. The hASCs were selected by plastic adherence approximately 5 d after isolation. For both cell lineages cell culture medium was changed 48 h after initial plating and every 3 d thereafter. The hAMECs cultures in 0.7% gelatin-coated flasks were at 90% confluence 7d postisolation. Both cell types were harvested with Tryple select (Invitrogen, U.S.).

3. Flow Cytometry. The hASCs and hAMECs (both at P0) were resuspended in a 3% BSA solution and incubated at room temperature for 20 min with fluorescent labeled antibodies. hASCs were incubated with mouse antihuman antibodies CD105-FITC, CD73-PE, CD90-APC, CD45-FITC, CD34-PE, and CD31-APC, and hAMECs with mouse-anti human CD31-APC, HLA-DR, and CD34-PE antibodies (all BD Biosciences, Germany) at manufacturer recommended concentrations. Cells

were subsequently washed with PBS, centrifuged, fixed with 1% paraformaldehyde, and analyzed in a FACs Calibur Flow Cytometer (BD Biosciences, U.S.) using the CELLQuest software V3.3.

4. Matrigel Assay. hAMECs were seeded at a concentration of 1.5×10^4/per well on Matrigel (BD Biosciences, U.S.) prepared in 96-well plates and incubated in EGM-2MV at 37 °C in a humidified incubator with 5% CO_2 for 20 h. Viable cells were then identified with calcein-AM (Invitrogen, USA), and their organization was visualized under an inverted microscope (Zeiss, Germany) and an Axioplan Imager Z1M microscope (Zeiss, Germany). Images were acquired and processed with AxioVision V.4.8 software (Zeiss, Germany).

5. Uptake of Acetylated Low-Density Lipoprotein (Dil-Ac-LDL). To assess Dil-AC-LDL uptake, hAMECs were cultured in 0.7% gelatin-coated polystyrene coverslips. Upon reaching confluence, cells were incubated for 4 h at 37 °C with 5% CO_2 in EGM-2MV containing 5 μg/mL of Dil-AC-LDL (Invitrogen, U.S.). After being washed with PBS and fixed in 3.7% (v/v) buffered formalin (Sigma, U.S.) for 1 h at room temperature, hAMECs nuclei were stained with 4′,6-diamidino-2-phenylindole (DAPI, Invitrogen, U.S.), and samples were visualized under a AXIOIMAGER Z1M (Zeiss) microscope, using axiovision software.

6. Preparation of the Constructs. Two different types of constructs, one with hASCs entrapped (homotypic) and one with cocultured hASCs and hAMECs (heterotypic), were prepared *in vitro*. To obtain homotypic spongy-like hydrogels, hASCs were ressuspended in α-MEM medium in a concentration of 1×10^7 cell/mL. The heterotypic spongy-like hydrogels were prepared with heterotypic cell suspension combining hASCs (1×10^6 cell/mL) and hAMECs (5×10^6 cell/mL). For both constructs, 100 μL of respective cell suspension was added to the GG-HA dried network structures. Constructs were incubated at 37 °C and 5% CO_2 for 30 min to increase cell entrapment. Constructs were cultured *in vitro* for 2 d prior to *in vivo* implantation in α-MEM medium and EGM-2MV (2 mL/per well).

7.. *In Vivo* Implantation in Mouse Excisional Wound Healing Model. Sixty-four Swiss Nu/Nu male mice (Charles River Laboratories, France) were randomly divided into four groups, comprising the experimental GG-HA spongy-like hydrogel (spongy-like hydrogel), GG-HA spongy-like hydrogel with hASCs (homotypic), GG-HA spongy-like hydrogel with hASCs and hAMECs (heterotypic), and the control group (control) without any material implanted. This study was conducted after approval by Direcção-Geral de Alimentação e Veterinária (DGAV), the Portuguese National Authority for Animal Health, and all the surgical/necropsy procedures were performed according to the applicable national regulations that comprise international animal welfare rules. Four animals were used per condition and per time point (3, 7, 14, and 21 d). Mice were anaesthetised with a mixture of Imalgene (ketamine) (75 mg/kg) (Merial Portuguesa, Portugal) plus Domitor (medetomidine) (1 mg/kg) (Esteve Farma, LDA, Portugal). A 1.2 cm diameter full-thickness excision was performed in each mouse at approximately 0.5 cm caudal to the intrascapular region. Spongy-like hydrogel constructs were placed on top of the wounds, which were covered with transparent dressing Hydrofilm (Hartmann, U.K.) and a final set of bandages. A subcutaneous injection of Depomedrol (20 mg/kg BW) (Pfizer, Portugal) was applied to the animals at days 0, 7, and 14, to delay wound healing.[42] Mice were maintained in separated compartments throughout the experiments and were euthanized by CO_2 inhalation at the referred time points, and explants were obtained for histological analysis.

8. Histological Procedure. Skin explants were collected at days 3, 7, 14, and 21, fixed in 10% formalin and embedded in paraffin. Representative sections were stained following routine protocols for H&E and Masson's trichrome. Sections were analyzed with a Axioplan Imager Z1m microscope, and images were acquired and processed with AxioVision V.4.8 software.

9. Immunolabeling. Immunostaining of hAMECs cultured in gelatin-coated coverslips, homotypic and heterotypic spongy-like hydrogel constructs, and histological sections of *in vivo* explants were performed after fixation with 3.7% (v/v) buffered formalin, permeabilization with 0.2% TritonX-100 and blocking with 3% Bovine Serum Albumin (BSA) (Sigma, U.S.). Regarding paraffin embedded samples, sections were rehydrated, and antigen retrieval was performed with Tris-EDTA (ethylenediaminetetraacetic acid) buffer (10 mM Tris Base, 1 mM EDTA Solution, 0.05% Tween 20, pH 9.0) (all Sigma, U.S.) before permeabilization and blocking. Primary antibodies CD31 (mouse antihuman, 1:30, Dako, Denmark), von Willebrand factor (vWF) (rabbit antihuman/mouse, 1:200, Dako, Denmark), CD31 (rabbit antihuman/mice, 1:20, Abcam, U.K.), tagged secondary antibodies, rabbit antimouse Alexafluor 594, and donkey antirabbit Alexafluor 488 (1:500, invitrogen, U.S.) were used. VECTASTAIN Elite ABC Kit (Vector Laboratories, U.S.) was further employed for the detection of CD31, according to manufacturer's instructions. Nuclei were stained either with DAPI (Invitrogen, U.S.) or Mayer's hematoxylin.

Phalloidin-TRITC (Sigma, U.S.) was used to stain cytoskeleton F-actin fibers in GG-HA spongy-like hydrogel constructs prior to implantation. AXIOIMAGER Z1M or Olympus Fluoview FV1000 laser confocal microscope (Olympus, Japan) were used for visualization of the samples.

10. Quantification of Collagen and Noncollagenous Proteins. Sirius Red/Fast Green Collagen Staining Kit (Chondrex, Inc., U.S.) was used to quantify the amount of collagen and noncollagenous proteins in the histological sections of 21 d postoperative *in vivo* explants following manufacturer instructions. Briefly, after being deparifinized and rehydrated, sections were incubated with the solution of dye at room temperature for 30 min. Afterward, sections were rinsed with water to eliminate excess dye. Dye extraction solution was added until the color was eluted from the tissue section and OD was measured at 540 and 605 nm in a Synergy HT microplate reader (Biotek, U.S.).

11. Image Analysis. *11.1. Wound Closure Assessment.* The percentage of wound closure was calculated by analyzing the planimetric digital images taken at day 0, 7, 14, and 21 postimplantation for all four animals of each condition and time point, according to the following equation:

$$(\text{area of original wound} - \text{area of actual wound}) / (\text{area of original wound}) \times 100$$

Wound was considered completely closed when wound area was equal to zero.

11.2. Quantification of Vessels Density and Diameter. The number and diameter of vessels were quantified at days 7 and 14 postoperative in the CD31 stained samples. Quantification and measurement were performed in randomly selected five high-power fields of five nonconsecutive tissue sections per

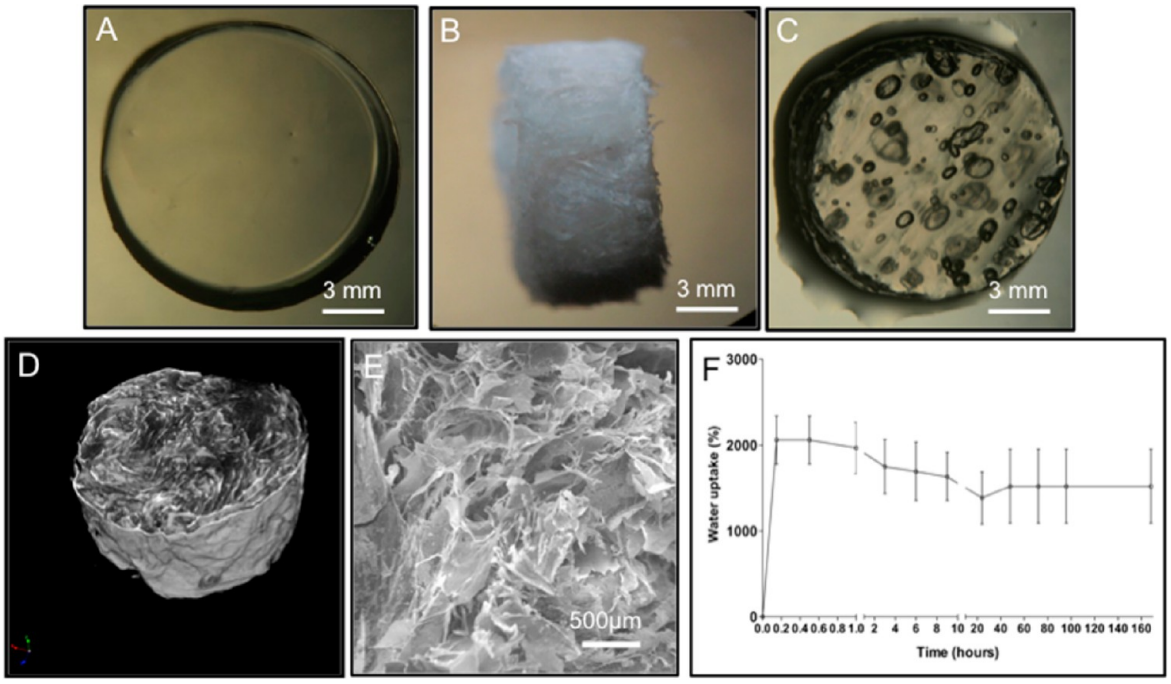

Figure 1. Properties of 2% GG-HA (A) hydrogel, (B, D, E) dried polymeric network and (C, F) spongy-like hydrogel. Macroscopic images of the GG-HA hydrogel (A) before and (B) after freeze-drying, and of the (C) respective spongy-like hydrogels formed after rehydration of the dried polymeric network with PBS. Microstructure, demonstrated by (D) μ-CT reconstruction and (E) SEM, and (F) water uptake profile of the dried polymeric network when rehydrated in cell culture medium.

A

	Expression of cell Surface Marker (%) (Mean±SD)						
Markers	CD73	CD105	CD90	CD45	CD34	CD31	HLA-DR
hAMECS	-	-	-	-	24.45 ± 4.29	90.39 ± 6.82	14.71 ± 11.92
hASCs	96,39 ± 0,76	98,90 ±0,52	93,96 ± 7,27	0,285 ± 0,08	0,655 ± 0,37	1,435 ± 1,46	0,03 ± 0,023

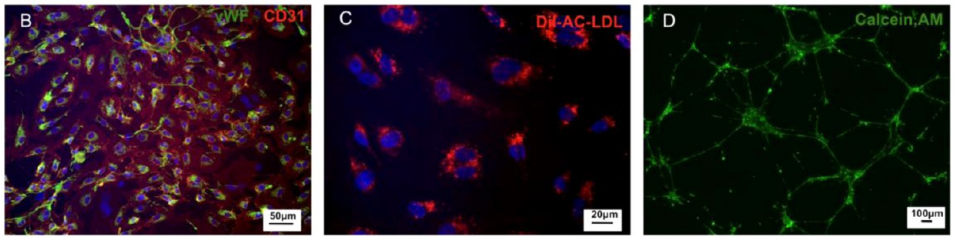

Figure 2. Phenotypic characterization of (A–D) freshly isolated and (E,F) entrapped hAMECs and hASCs. (A) Surface marker profile of hAMECs and hASCs pools at passage 0 obtained by flow cytometry analysis. Endothelial phenotype was confirmed by (B) the expression of CD31 (red) and vWF (green) by immunocytochemical analysis, and by their capacity to (C) uptake dil-AC-LDL (red) and (D) to form tubular-like structures on Matrigel remaining viable as confirmed by calcein-AM staining (green). SD: standard deviation.

time point and per animal within each group. Only vessels with a diameter of <50 μm[43] were considered. Mean results of the number of vessels per field are expressed as vessel density.

11.3. Dermal Differentiation. Newly formed skin quality was assessed after 21 d of implantation, through the quantification of the dermal differentiation on Masson's Trichrome-stained histological samples, according to criteria described by Sun et al.,[15] using the following criteria: grade 1, thin, dense, and monotonous fibrosis; 2, thicker but still dense and monotonous fibrosis; 3, two layers but not completely discrete; 4, two discrete layers with superficial fibrosis and loose alveolar tissue within the deep layer.

11.4. Epidermal Thickness Quantification. The epidermal thickness was measured on H&E stained histological sections, of both experimental and control groups, explanted at day 21. Four tissue sections per animal within each group were examined after a random selection of five high-power fields per section and by performing five measurements of the epidermal thickness per field.

12. Statistic Analysis. Statistical analysis of wound closure was performed using two-way ANOVA with Bonferroni post-tests, while for vessels diameter kruskal-wallis test, with Dunns post test was used. For vessel number, epidermal thickness, epithelial maturation, and dermal differentiation one-way ANOVA with Tukey's post-tests was employed (GraphPad

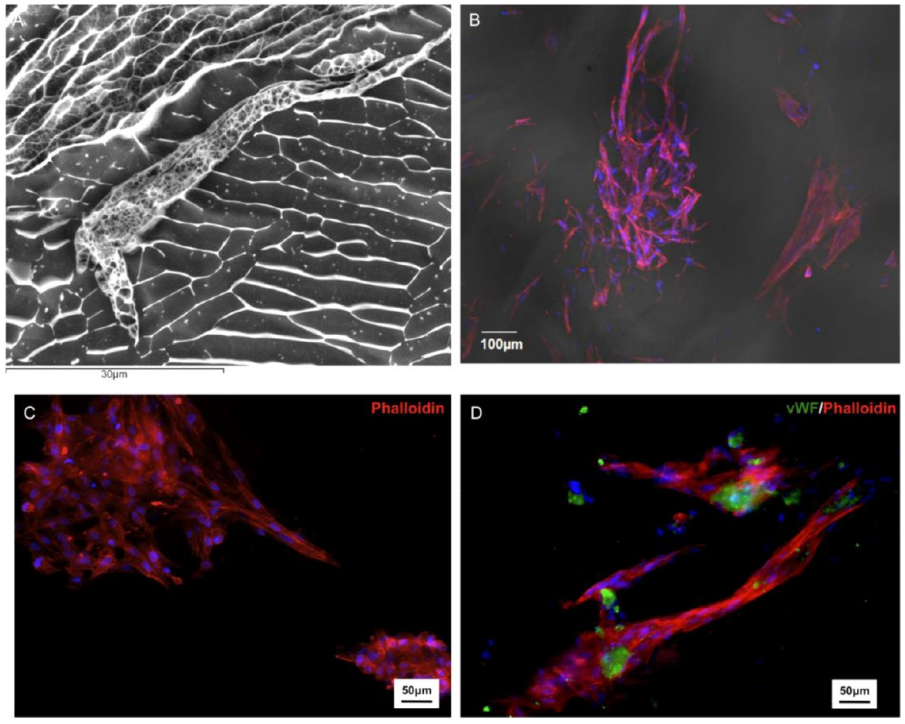

Figure 3. Organization of (A−C) hASCs and (D) hASCs cocultured with hAMECs within the 2% GG-HA spongy-like hydrogels after 2 d of culture. The organization of the cells demonstrated by (A) cryo-SEM, (B) confocal microscopy, and (C, D) fluorescence microscopy after cytoskeletal F-actin fibers staining with rhodamine-labeled phalloidin (red). (B−D) Cytoskeleton organization confirmed hASCs spreading while (D) the expression of vWF (green) showed the interaction of the hAMECs with the hASCs. Nuclei were stained with DAPI (blue).

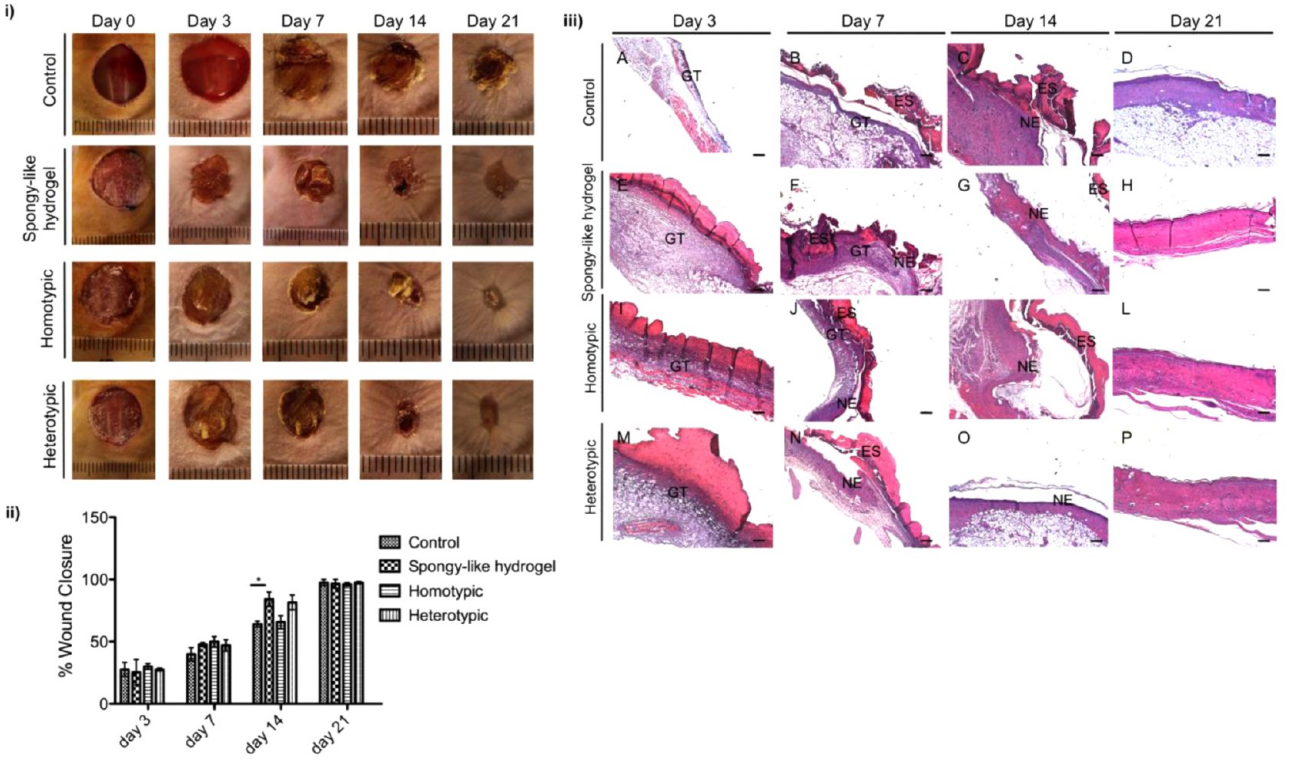

Figure 4. Evaluation of the effect of acellular, homotypic, and heterotypic 2% GG-HA spongy-like hydrogels over wound closure. (i) Representative macroscopic images of the wounds and (ii) respective percentage of wound closure up to 21 d post-transplantation. (iii) Representative images of H&E-stained explants of (A−D) acellular, (E−H) homotypic, and (I−L) heterotypic spongy-like hydrogels, and (M−P) control groups at days (A, E, I, M) 3, (B, F, J, N) 7, (C, G, K, O) 14, and (D, H, L, P) 21, highlighting wound healing progression. Scale bar corresponds to 200 μm. GT − granulation tissue, ES − eschar, and NE − neoepidermis. *$p < 0.05$.

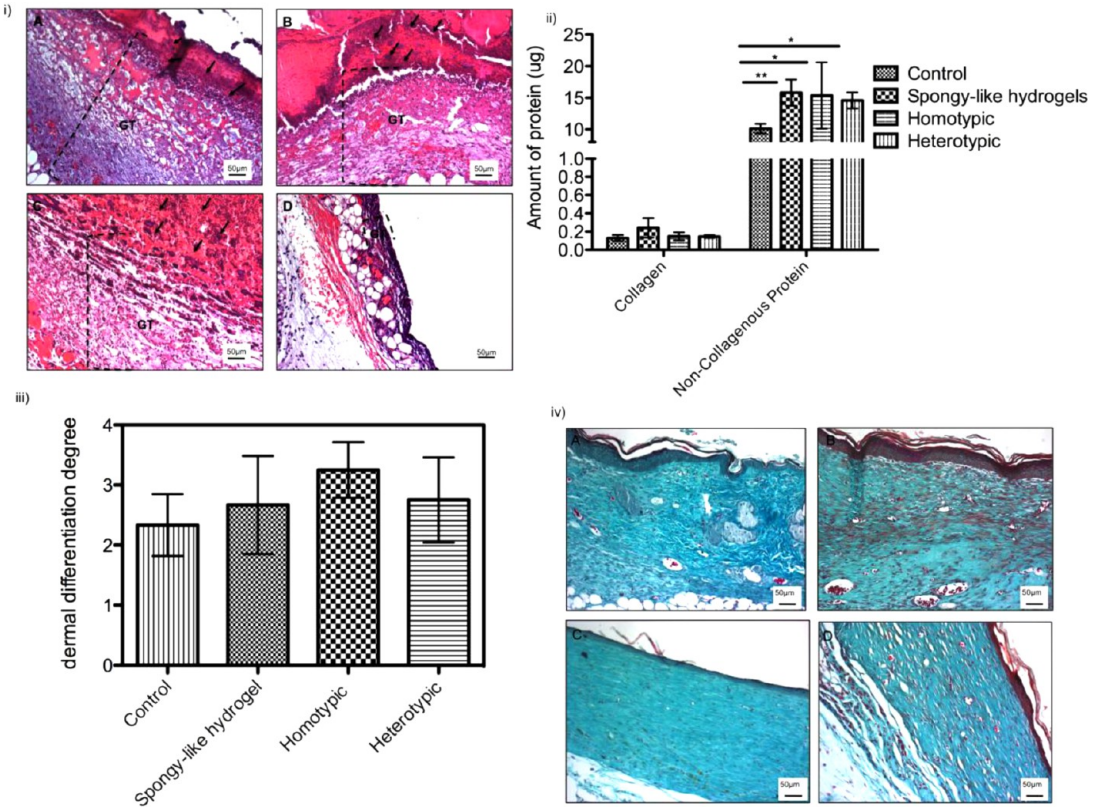

Figure 5. (i) Tissue reaction 3 d after transplantation of (A) acellular, (B) homotypic, and (C) heterotypic spongy-like hydrogels revealing the absorption of the exudates by the spongy-like hydrogels (arrows) and significant granulation tissue (GT, limited by the dashed line) formation. (D) Represents the control condition. Graphical representation of the (ii) amount of collagen and noncollagenous proteins quantified by sirius red/fast green assay, and (iii) dermal differentiation degree obtained after a graded qualitative analysis[15] of (iv) Masson's Trichrome stained histological tissue samples of the different test groups at day 21. $*p < 0.05$, $**p < 0.01$.

Prism 4.02). Significance levels, determined using post tests between negative control and the three experimental groups, were set at $*p < 0.05$, $**p < 0.01$, and $***p < 0.001$.

RESULTS

1. Gellan Gum-Hyaluronic Acid Spongy-like Hydrogel Constructs: Elements Properties and in Vitro Assembling. GG-HA spongy-like hydrogels have been previously proposed[39,40] as cell-adhesive structures generated through a sequential processing method that includes stabilization, freezing, freeze-drying, and rehydration. GG-HA hydrogels (Figure 1A) were freeze-dried giving rise to dried polymeric networks (Figure 1 B) that in turn originated spongy-like hydrogels after rehydration with any saline solution, as for example PBS (Figure 1 C). The dried polymeric networks presented a highly interconnected porous microstructure with a pore size between 11.32 and 509.36 μm, as depicted by μ-CT (Figure 1D) and SEM (Figure 1E) analysis. Moreover, those structures were able to uptake about 2000% of water within 15 min when hydrated with culture medium (Figure 1 F) thus forming the spongy-like hydrogels. The hydration equilibrium in cell culture medium was reached after 20 h of incubation, at which time the spongy-like hydrogels presented ~1500% of water content (Figure 1F). Moreover, spongy-like hydrogels retain the attractive features of hydrogels and present advantages in relation to standard hydrogels that render them as interesting soft tissues ECM analogues.[39,40]

The phenotype of both the hASCs and hAMECs populations at passage 0, isolated from the same lipoaspirate sample and used to create the constructs, was analyzed to confirm the respective mesenchymal and endothelial phenotypes. After flow cytometry analysis the expression of CD105, CD90, and CD73 by more than 90% of the hASCs and the neglectable expression of CD34, CD45, and CD31 markers was confirmed (Figure 2A). Furthermore, ~90% of the hAMECs population expressed the CD31 endothelial characteristic marker (Figure 2A). The endothelial phenotype of the hAMECs was further confirmed by the coexpression of CD31 and vWF by immunocytochemistry (Figure 2B), as well as by the ability of the cells to uptake Dil-AC-LDL (Figure 2C) and to form tubular-like structures on matrigel remaining viable, as confirmed by calcein-AM staining (Figure 2D). In what concerns the expression of HLA-DR, while its expression was absent in the hASCs population, ~15% of the hAMECs were positive for that marker (Figure 2A).

Replicates of the constructs formed by hydration of the GG-HA dried polymeric networks at the time of seeding, thus entrapping/encapsulating the respective cells, were analyzed after the *in vitro* culture aiming at providing insight on the interaction of the cells with the matrix and consequent arrangement prior implantation. Two days after entrapment, hASCs were adhered to the pore walls of the spongy-like hydrogel, as observed by cryo-SEM technique (Figure 3A). This cellular interaction with the polymeric structure was further evidenced in confocal microscopy images, where the embossment of the shape of the cells on the material surface was clearly visualized (Figure 3B). Moreover, hASCs exhibited their typical fibroblast-like morphology with an organized cytoskeleton in both homotypic (Figure 3C) and heteroptypic

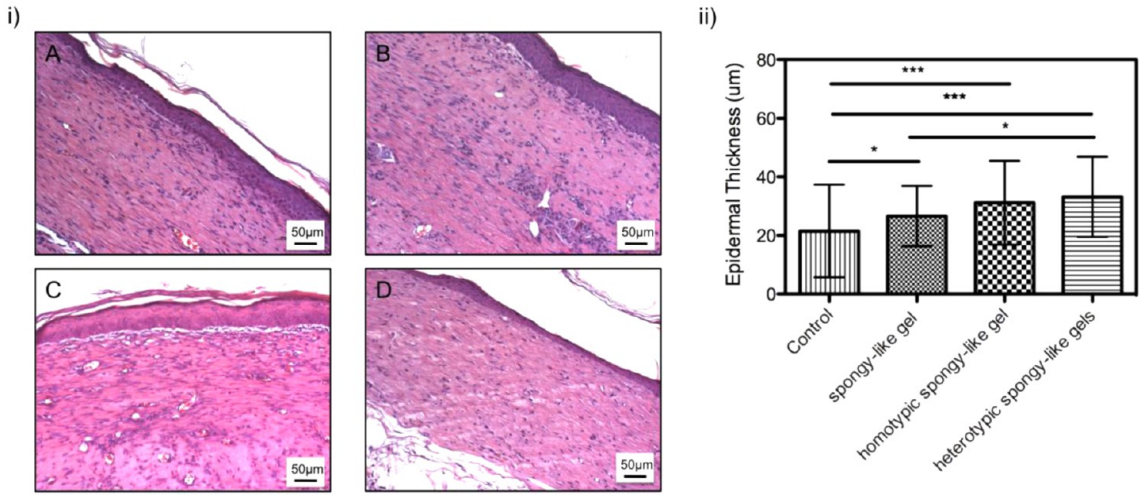

Figure 6. Neoepidermis analysis. (i) H&E representative micrographs of the 21 d explants of (A) acellular, (B) homotypic, and (C) heterotypic spongy-like hydrogels, and (D) control groups. (ii) Representation of the thickness of the epidermis for the different experimental groups indicating the differences among them. *$p < 0.05$, ***$p < 0.001$.

constructs (Figure 3D), while hAMECs, identified by vWF staining in the heterotypic construct, were found to interact with hASCs but not with the matrix (Figure 3D).

2. Wound Healing Progression. Wound closure macroscopic/qualitative analysis (Figure 4i) and quantification (Figure 4ii) performed along the implantation time allowed the assessment of the influence of the different test groups over wound closure rate. The percentage of wound closure was slightly higher in experimental groups than in the control at days 7 and 14, though a significant difference ($p < 0.05$) was only detected for the spongy-like hydrogel condition at day 14 postoperative (Figure 3ii). Nonetheless, wounds were progressively closing in all the conditions reaching complete closure at day 21 postoperative. The evolution of the wound healing process followed after H&E staining revealed several differences between the test groups (Figure 4iii) as confirmed by the detailed assessment of granulation tissue formation (Figure 5i), neodermis (Figure 5ii–iv), and neoepidermis formation (Figure 6) and revascularization (Figure 7). At day three, an exuberant granulation tissue was observed in both acellular and cellular experimental groups (Figure 5i,A–C) but not in the control condition (Figure 5i,D). In the experimental conditions, the exudate that was formed upon transplantation as a consequence of the inflammatory process (Figure 4iii,E,I,M) was absorbed by the spongy-like hydrogels (Figure 5i,A–C). The higher volume of granulation tissue, early produced in the experimental groups, is correlated to a significantly higher ($p < 0.05$) amount of protein detected in the subsequently formed neodermis of experimental groups in comparison to control (Figure 5ii), but not to the dermal differentiation degree (Figure 5iii). Although it seems that the control group exhibited a less-differentiated dermis than the experimental groups, this difference was not statistically significant. This was also confirmed by the masson trichrome staining (Figure 5iv).

A complete re-epithelialization of the wounds was observed for all the conditions tested at the end time point (Figure 4iii,D,H,L,P). Nonetheless, the thickness of the neoepidermis formed varied among the test groups (Figure 6). All the spongy-like hydrogels groups showed a significantly thicker ($p < 0.05$) epidermis than the control group. Moreover, heterotypic spongy-like hydrogel group showed a significantly thicker epidermis ($p < 0.05$) than the acellular spongy-like hydrogel group (Figure 6ii).

2.1. Neovascularization. The impact of the acellular spongy-like hydrogels, and homotypic and heterotypic constructs, over neotisssue vascularization was analyzed by determining the density of the vessels at different time points. Heterotypic spongy-like hydrogels led to the formation of a significantly higher ($p < 0.05$) number of vessels in comparison to control, both at 7 and 14 d. In addition, the acellular and the homotypic spongy-like hydrogels, as well as the control groups, presented similar results in terms of vessel density at day 7. However, at day 14 the number of vessels detected for the acellular spongy-like hydrogel group was significantly higher ($p < 0.05$) than it was for the control but significantly lower ($p < 0.05$) than it was for the heterotypic spongy-like hydrogel (Figure 7i,A,B). The contribution of the hAMECs present in the heterotypic spongy-like hydrogel toward the tissue neovascularization was further confirmed by the detection of specific human CD31 positive cells incorporating the vessels at day 21 (Figure 7ii,A,B).

DISCUSSION

The limitations of current skin substitutes have led the demand for improved solutions. Tissue engineering is expected to answer to those requirements with the creation of superior constructs comprising specific features. In this study, we propose GG-HA spongy-like hydrogel-based constructs, in which the role of adipose tissue cells is potentiated by their interaction with the ECM-like analogue, to improve the neovascularization of full-thickness excisional wounds. Moreover, the proposed approach combines *off-the-shelf* 3D structures with two types of cells obtained from an abundant cell source, as a way to diminish the production time of the constructs. Excised fat was used as a single-cell source, allowing not only the simultaneous isolation from an accessible tissue of both hASCs and microvascular endothelial cells under standard conditions but also in sufficient yields,[44] avoiding the need of extensive culture. A yield of $\sim 160 \times 10^5$ nucleated cells/mL of lipoaspirate was achieved usually from a total volume of the sample in the range of 150–350 mL. Considering the percentage of hASCs and hAMECs within the adipose tissue

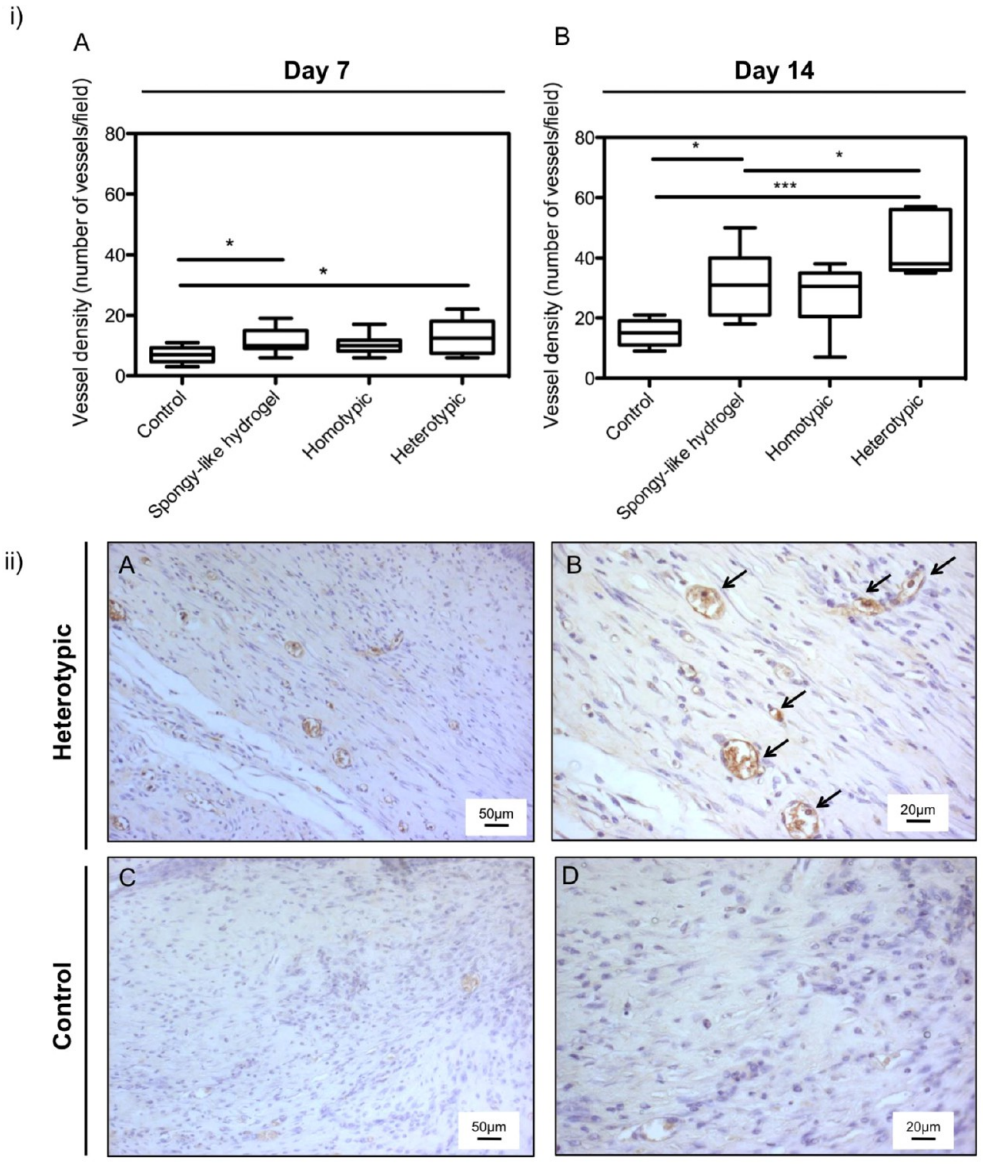

Figure 7. Effect of the spongy-like gels-based constructs over neotissue vascularization. (i) Representation of the density of vessels, quantified in the wounded area at days (A) 7 and (B) 14 postimplantation.after CD31 staining. (ii) Immunolocalization of human endothelial CD31 positive cells in the heterotypic spongy-like hydrogel group at day 21 postoperative. (B, D) Higher magnification images of A and C, respectively. (C, D) The immunostaining negative controls. $*p < 0.05$; $***p < 0.00$.

SVF (data not published consistent with the literature[45]), a yield of ~4−16 × 10^6 hASCs and ~2.5−10 × 10^6 hAMECs per sample was attained.

A suitable 3D structure capable of providing an adequate microenvironment that supports cell physiological maintenance and potentiates the dynamics of cellular interactions is crucial to accomplish the aim of tissue engineering strategies. Spongy-like hydrogels, formed by a sequential processing that comprises the formation of a precursor hydrogel, stabilization, freeze, freeze-drying, and rehydration, possess intrinsic cell adhesive properties. Moreover, issues such as adverse cross-linking conditions that might compromise the encapsulated cells and that have been posed as a limiting factor for different hydrogels[46] are avoided. In fact, GG spongy-like hydrogels are obtained from stable polymeric dried networks upon a simple rehydration procedure with any saline solution, including a cell suspension in culture medium.[39] Thus, cells become entrapped and then adhere to the material without being subjected to any adverse conditions. These cell adhesive features are potentiated by the conjugation of the significantly lower water content and a microstructural rearrangement that occur during the processing, which is characterized by pore wall thickening (70 μm) and pore size augmentation (100 to 500 μm compared with ~20 μm in precursor GG hydrogels).[39,40] Moreover, the lower water content in relation to the precursor hydrogels was also shown to influence cell adhesion by enhancing protein absorption. These features allow surpassing the limitations on the lack of cell adhesion characteristic of the majority of hydrogels,[47−49] including GG hydrogels to which the combination with gelatin[17,50] and the modification with a GRGDS peptide sequence[12] were the only routes capable of conferring cell adhesive features. Except for the protein-derived[51−53] or cell-adhesive modified hydrogels,[3,13−17] the lack of cell-adhesive sites in the majority of hydrogels[47,49] restrains cells to perform in their maximum level and has been reducing their use to acellular strategies.[15,54] Additionally,

spongy-like hydrogels present features of both sponges and hydrogels and thus an enhanced flexibility and rapid recovery after the application of a compressive strain, when compared with the respective hydrogels.[40] GG-based spongy-like hydrogels compressive modulus ranging from 10 to 40 kPa, depending on the concentration and type of polymers,[39,40] closely meet the values reported for human skin (13.2−33.4 kPa).[55] These properties not only allow surpassing common mechanical limitations of hydrogels but also permit a superior handling for transplantation. Furthermore, spongy-like hydrogels maintain the water retention capacity characteristic of hydrogels providing a unique aqueous microenvironment that is crucial for a better healing.[13]

The progression of wound closure in the presence of spongy-like hydrogels revealed an accelerated process suggesting the beneficial role of the GG-HA spongy-like hydrogels. The early integration of the spongy-like hydrogels into the wounds not only proved to be successful but also contributed to the formation of significant amounts of granulation tissue. Moreover, due to their hygroscopic nature, the inflammatory exudate was absorbed by the materials, which has contributed to the rapid degradation of the materials, almost not found at day 14 and completely absent at day 21. This progressive degradation of the spongy-like hydrogel together with the early granulation tissue formation, a fundamental template within the wound healing cascade,[56] appears to play a significant role in the progression of the healing and in the neoepidermis formation and neovascularization, but not in neodermal organization. This is in accordance with previous works that highlighted the relevance of the capacity of absorbing wound exudate by dextran hydrogels,[15] chondroitin sulfate, and HA[61] for an enhanced wound healing. All the spongy-like hydrogel groups showed a significantly thicker epidermis than the control group. Moreover, although the quality of the deposited neodermis did not vary between the control and the conditions with the spongy-like hydrogels, a significantly higher amount of noncollagen proteins, such as fibronectin, laminin, proteoglycans, and elastin, which are known to be major multifunctional components of skin ECM,[57] was detected for the experimental groups. An enhanced number of vessels was also observed in the wounded area with the spongy-like hydrogels, except for the homotypic construct, in comparison to the control. Although we are not able to provide evidence of what is occurring *in vivo*, GG-HA spongy-like hydrogels lost ∼50% of their mass *in vitro* after 21 d in the presence of hyaluronidase (data not shown). Therefore, we assumed that along the time of implantation, HA fragments are released to the wound matrix. Low molecular weight HA fragments, which have been described to play an important role not only in tissue integrity maintenance but also in wound healing[58] promoting cellular differentiation and angiogenesis[59,60] are likely to be present thus influencing the neovascularization, as noticed by the higher density of vessels detected at early time points for the acellular condition.

It might also be speculated that the infiltration of the inflammatory exudate into the GG-HA spongy-like hydrogels has promoted a faster and closer interaction between the transplanted and the host cells. In opposition to the importance of the absorption of the inflammatory exudate, previous works[1561] have not referred to this phenomenon. The generated spongy-like hydrogel-based constructs, maintained in culture *in vitro* for 2 d prior to implantation, have been shown to support hASCs adhesion in agreement with previous observations[39] and, in the case of the heterotypic GG-HA spongy-like hydrogels, to allow the interaction between hASCs and hAMECs. Upon transplantation, the effect of the cellular elements was noticed not only in the neovascularization, as hypothesized, but also in the epidermal thickness. Heterotypic spongy-like hydrogels lead to the formation of an epidermis with increased thickness in relation to the acellular spongy-like hydrogel. This is likely related to findings reported by other authors[61] demonstrating that transplanted endothelial cells lead to increased KCs migration and consequently to enhanced re-epithelialization. The effect of the presence of cells within the GG-HA constructs over the vessel density at early time points was only observed for the heterotypic constructs. This was expected and in agreement with works that have shown that matrices and scaffold prevascularization, taking advantage of progenitor or endothelial cells,[29−31,51] is one of the most promising strategies to promote vascularization *in vivo*. Furthermore, knowing that MSCs are identical to pericytes,[62,63] which play a role in vascular stabilization,[64] the interaction between hAMECs and hASCs in the heterotypic construct was also expected to impact neotissue vascularization and confirmed by the higher density of vessels detected for that condition. The combined influence of spongy-like hydrogel and the exogenous cells in promoting neovascularization was further reinforced through the detection of the transplanted endothelial cells in the neovessels. Contrarily, the results for the homotypic constructs were unforeseen. Although the role of hASCs in angiogenesis has been stressed by showing that these cells are capable of secreting angiogenic factors affecting endothelial cells behavior *in vitro*[65] and impacting the neovasculature,[66] its interaction with the GG-HA spongy-like hydrogels might have conditioned the hASCs signaling cascade. Future studies capable of revealing the potential modulation of the hASCs angiogenic secretome by GG-based spongy-like hydrogels will be of major interest for the design of improved strategies.

CONCLUSIONS

Altogether, our findings showed that GG-HA spongy-like hydrogels provided the environment for cells to respond to the host signals and to reach the wound bed in a timely fashion and in sufficient number to maximize their effects over neotissue vascularization. Thus, a synergistic effect of the GG-HA structure and adipose tissue cells was demonstrated. A tissue-engineered construct based on a prevascularized GG-HA spongy-like hydrogel is herein proposed to promote full-thickness skin wound regeneration by improving neotissue vascularization. Microvascular endothelial cells and hASCs, obtained in high yields from an abundant and easily accessible tissue, in combination with an off-the-shelf dried polymeric network as an integrated construct, tackle the need for a reduced production time. The proposed GG-HA spongy-like hydrogel was able to meet quality regeneration parameters such as fast wound closure and re-epithelialization, a distinct dermal matrix remodelling, and improved neovascularization. A cumulative effect of the GG-HA spongy-like hydrogel matrix and the hAMECs integrated in the heterotypic constructs maximized neovessel formation and the integration of the transplanted cells into the new vasculature.

AUTHOR INFORMATION

Corresponding Author

*E-mail: apmarques@dep.uminho.pt.

Notes

The authors declare no competing financial interest.

■ ACKNOWLEDGMENTS

Work developed at 3B's Research Group, University of Minho. We would like to thank Hospital da Prelada (Porto), in particular, Dr. P. Costa for lipoaspirates collection. Financial support by Skingineering (PTDC/SAU-OSM/099422/2008), Portuguese Foundation for Science and Technology (FCT) funded project, is also acknowledged. The research leading to these results has received funding from the European Union's Seventh Framework Programme (FP7/2007-2013) under Grant No. REGPOT-CT2012-316331-POLARIS.

■ ABBREVIATIONS

GG-HA = gellan gum-hyaluronic acid
hASCs = human adipose stem cells
hAMECs = human adipose microvascular endothelial cells
MSCs = mesenchymal stem cells
SVF = stromal vascular fraction
Dil-AC-LDL = acetylated low-density lipoprotein

■ REFERENCES

(1) Yannas, I. V.; Lee, E.; Orgill, D. P.; Skrabut, E. M.; Murphy, G. F. Synthesis and Characterization of a Model Extracellular Matrix That Induces Partial Regeneration of Adult Mammalian Skin. *Proc. Natl. Acad. Sci. U.S.A.* **1989**, *86*, 933−937.

(2) Gaspar, A.; Moldovan, L.; Constantin, D.; Stanciuc, A. M.; Sarbu Boeti, P. M.; Efrimescu, I. C. Collagen-Based Scaffolds for Skin Tissue Engineering. *J. Med. Life* **2011**, *4*, 172−177.

(3) Helary, C.; Bataille, I.; Abed, A.; Illoul, C.; Anglo, A.; Louedec, L.; Letourneur, D.; Meddahi-Pelle, A.; Giraud-Guille, M. M. Concentrated Collagen Hydrogels as Dermal Substitutes. *Biomaterials* **2010**, *31*, 481−490.

(4) Caravaggi, C.; De Giglio, R.; Pritelli, C.; Sommaria, M.; Dalla Noce, S.; Faglia, E.; Mantero, M.; Clerici, G.; Fratino, P.; Dalla Paola, L.; Mariani, G.; Mingardi, R.; Morabito, A. Hyaff 11-Based Autologous Dermal and Epidermal Grafts in the Treatment of Noninfected Diabetic Plantar and Dorsal Foot Ulcers: A Prospective, Multicenter, Controlled, Randomized Clinical Trial. *Diabetes Care* **2003**, *26*, 2853−2859.

(5) Wang, T. W.; Sun, J. S.; Wu, H. C.; Tsuang, Y. H.; Wang, W. H.; Lin, F. H. The Effect of Gelatin-Chondroitin Sulfate-Hyaluronic Acid Skin Substitute on Wound Healing in Scid Mice. *Biomaterials* **2006**, *27*, 5689−5697.

(6) Ahmed, T. A.; Dare, E. V.; Hincke, M. Fibrin: A Versatile Scaffold for Tissue Engineering Applications. *Tissue Eng., Part B* **2008**, *14*, 199−215.

(7) Haslik, W.; Kamolz, L. P.; Nathschlager, G.; Andel, H.; Meissl, G.; Frey, M. First Experiences with the Collagen-Elastin Matrix Matriderm as a Dermal Substitute in Severe Burn Injuries of the Hand. *Burns* **2007**, *33*, 364−368.

(8) Sanders, J. E.; Stiles, C. E.; Hayes, C. L. Tissue Response to Single-Polymer Fibers of Varying Diameters: Evaluation of Fibrous Encapsulation and Macrophage Density. *J. Biomed. Mater. Res.* **2000**, *52*, 231−237.

(9) Ng, K. W.; Hutmacher, D. W.; Schantz, J. T.; Ng, C. S.; Too, H. P.; Lim, T. C.; Phan, T. T.; Teoh, S. H. Evaluation of Ultra-Thin Poly(Epsilon-Caprolactone) Films for Tissue-Engineered Skin. *Tissue Eng., Part A* **2001**, *7*, 441−455.

(10) van Dorp, A. G.; Verhoeven, M. C.; Koerten, H. K.; van Blitterswijk, C. A.; Ponec, M. Bilayered Biodegradable Poly(Ethylene Glycol)/Poly(Butylene Terephthalate) Copolymer (Polyactive) as Substrate for Human Fibroblasts and Keratinocytes. *J. Biomed. Mater. Res.* **1999**, *47*, 292−300.

(11) Lutolf, M. P.; Hubbell, J. A. Synthetic Biomaterials as Instructive Extracellular Microenvironments for Morphogenesis in Tissue Engineering. *Nat. Biotechnol.* **2005**, *23*, 47−55.

(12) Silva, N. A.; Cooke, M. J.; Tam, R. Y.; Sousa, N.; Salgado, A. J.; Reis, R. L.; Shoichet, M. S. The Effects of Peptide Modified Gellan Gum and Olfactory Ensheathing Glia Cells on Neural Stem/Progenitor Cell Fate. *Biomaterials* **2012**, *33*, 6345−6354.

(13) Wong, V. W.; Rustad, K. C.; Galvez, M. G.; Neofytou, E.; Glotzbach, J. P.; Januszyk, M.; Major, M. R.; Sorkin, M.; Longaker, M. T.; Rajadas, J.; Gurtner, G. C. Engineered Pullulan-Collagen Composite Dermal Hydrogels Improve Early Cutaneous Wound Healing. *Tissue Eng., Part A* **2010**, *17*, 631−644.

(14) Tran, N. Q.; Joung, Y. K.; Lih, E.; Park, K. D. In Situ Forming and Rutin-Releasing Chitosan Hydrogels as Injectable Dressings for Dermal Wound Healing. *Biomacromolecules* **2011**, *12*, 2872−2880.

(15) Sun, G.; Zhang, X.; Shen, Y. I.; Sebastian, R.; Dickinson, L. E.; Fox-Talbot, K.; Reinblatt, M.; Steenbergen, C.; Harmon, J. W.; Gerecht, S. Dextran Hydrogel Scaffolds Enhance Angiogenic Responses and Promote Complete Skin Regeneration During Burn Wound Healing. *Proc. Natl. Acad. Sci. U.S.A.* **2011**, *108*, 20976−20981.

(16) Luo, Y.; Diao, H.; Xia, S.; Dong, L.; Chen, J.; Zhang, J. A Physiologically Active Polysaccharide Hydrogel Promotes Wound Healing. *J. Biomed. Mater. Res., Part A* **2010**, *94*, 193−204.

(17) Shin, H.; Olsen, B. D.; Khademhosseini, A. The Mechanical Properties and Cytotoxicity of Cell-Laden Double-Network Hydrogels Based on Photocrosslinkable Gelatin and Gellan Gum Biomacromolecules. *Biomaterials* **2012**, *33*, 3143−3152.

(18) Lee, P. Y.; Cobain, E.; Huard, J.; Huang, L. Thermosensitive Hydrogel Peg-Plga-Peg Enhances Engraftment of Muscle-Derived Stem Cells and Promotes Healing in Diabetic Wound. *Mol. Ther.* **2007**, *15*, 1189−1194.

(19) Khademhosseini, A.; Langer, R. Microengineered Hydrogels for Tissue Engineering. *Biomaterials* **2007**, *28*, 5087−5092.

(20) Boyce, S. T. Design Principles for Composition and Performance of Cultured Skin Substitutes. *Burns* **2001**, *27*, 523−533.

(21) Metcalfe, A. D.; Ferguson, M. W. Bioengineering Skin Using Mechanisms of Regeneration and Repair. *Biomaterials* **2007**, *28*, 5100−5113.

(22) Laschke, M. W.; Harder, Y.; Amon, M.; Martin, I.; Farhadi, J.; Ring, A.; Torio-Padron, N.; Schramm, R.; Rucker, M.; Junker, D.; Haufel, J. M.; Carvalho, C.; Heberer, M.; Germann, G.; Vollmar, B.; Menger, M. D. Angiogenesis in Tissue Engineering: Breathing Life into Constructed Tissue Substitutes. *Tissue Eng., Part A* **2006**, *12*, 2093−2104.

(23) Cassell, O. C.; Hofer, S. O.; Morrison, W. A.; Knight, K. R. Vascularisation of Tissue-Engineered Grafts: The Regulation of Angiogenesis in Reconstructive Surgery and in Disease States. *Br. J. Plast. Surg.* **2002**, *55*, 603−610.

(24) Kannan, R. Y.; Salacinski, H. J.; Sales, K.; Butler, P.; Seifalian, A. M. The Roles of Tissue Engineering and Vascularisation in the Development of Micro-Vascular Networks: A Review. *Biomaterials* **2005**, *26*, 1857−1875.

(25) Sheridan, M. H.; Shea, L. D.; Peters, M. C.; Mooney, D. J. Bioabsorbable Polymer Scaffolds for Tissue Engineering Capable of Sustained Growth Factor Delivery. *J. Controlled Release* **2000**, *64*, 91−102.

(26) Tabata, Y.; Miyao, M.; Yamamoto, M.; Ikada, Y. Vascularization into a Porous Sponge by Sustained Release of Basic Fibroblast Growth Factor. *J. Biomater. Sci., Polym. Ed.* **1999**, *10*, 957−968.

(27) Supp, D. M.; Boyce, S. T. Overexpression of Vascular Endothelial Growth Factor Accelerates Early Vascularization and Improves Healing of Genetically Modified Cultured Skin Substitutes. *J. Burn Care Rehabil.* **2002**, *23*, 10−20.

(28) Supp, D. M.; Karpinski, A. C.; Boyce, S. T. Vascular Endothelial Growth Factor Overexpression Increases Vascularization by Murine but Not Human Endothelial Cells in Cultured Skin Substitutes Grafted to Athymic Mice. *J. Burn Care Rehabil.* **2004**, *25*, 337−345.

(29) Tonello, C.; Vindigni, V.; Zavan, B.; Abatangelo, S.; Abatangelo, G.; Brun, P.; Cortivo, R. In Vitro Reconstruction of an Endothelialized

Skin Substitute Provided with a Microcapillary Network Using Biopolymer Scaffolds. *FASEB J.* **2005**, *19*, 1546−1548.
(30) Chen, X.; Aledia, A. S.; Ghajar, C. M.; Griffith, C. K.; Putnam, A. J.; Hughes, C. C.; George, S. C. Prevascularization of a Fibrin-Based Tissue Construct Accelerates the Formation of Functional Anastomosis with Host Vasculature. *Tissue Eng., Part A* **2009**, *15*, 1363−1371.
(31) Wu, X.; Rabkin-Aikawa, E.; Guleserian, K. J.; Perry, T. E.; Masuda, Y.; Sutherland, F. W.; Schoen, F. J.; Mayer, J. E., Jr.; Bischoff, J. Tissue-Engineered Microvessels on Three-Dimensional Biodegradable Scaffolds Using Human Endothelial Progenitor Cells. *Am. J. Physiol.* **2004**, *287*, H480−487.
(32) Black, A. F.; Berthod, F.; L'Heureux, N.; Germain, L.; Auger, F. A. In Vitro Reconstruction of a Human Capillary-Like Network in a Tissue-Engineered Skin Equivalent. *FASEB J.* **1998**, *12*, 1331−1340.
(33) Wu, Y.; Chen, L.; Scott, P. G.; Tredget, E. E. Mesenchymal Stem Cells Enhance Wound Healing through Differentiation and Angiogenesis. *Stem Cells* **2007**, *25*, 2648−2659.
(34) Sasaki, M.; Abe, R.; Fujita, Y.; Ando, S.; Inokuma, D.; Shimizu, H. Mesenchymal Stem Cells Are Recruited into Wounded Skin and Contribute to Wound Repair by Transdifferentiation into Multiple Skin Cell Type. *J. Immunol.* **2008**, *180*, 2581−2587.
(35) Satoh, H.; Kishi, K.; Tanaka, T.; Kubota, Y.; Nakajima, T.; Akasaka, Y.; Ishii, T. Transplanted Mesenchymal Stem Cells Are Effective for Skin Regeneration in Acute Cutaneous Wounds. *Cell Transplant.* **2004**, *13*, 405−412.
(36) Fu, X.; Fang, L.; Li, X.; Cheng, B.; Sheng, Z. Enhanced Wound-Healing Quality with Bone Marrow Mesenchymal Stem Cells Autografting after Skin Injury. *Wound Repair Regener.* **2006**, *14*, 325−335.
(37) Gimble, J. M.; Katz, A. J.; Bunnell, B. A. Adipose-Derived Stem Cells for Regenerative Medicine. *Circ. Res.* **2007**, *100*, 1249−1260.
(38) Cerqueira, M. T.; Pirraco, R. P.; Santos, T. C.; Rodrigues, D. B.; Frias, A. M.; Martins, A. R.; Reis, R. L.; Marques, A. P. Human Adipose Stem Cells Cell Sheet Constructs Impact Epidermal Morphogenesis in Full-Thickness Excisional Wounds. *Biomacromolecules* **2013**, *14*, 3997−4008.
(39) da Silva, L. C.; Cerqueira, M.T.; Marques, A. P.; Correlo, V. M.; Sousa, R. A.; Reis, R. L. *Gellan Gum-Based Spongy-Like Hydrogels: Methods and Biomedical Applications Thereof;* 2013; WO 2014/167513; PCT/IB2014/060563.
(40) da Silva, L. C.; Cerqueira, M.T.; Sousa, A. R.; Reis, R. L.; Correlo, V. M.; Marques, A. P. Engineering Cell-Adhesive Gellan Gum Spongy-Like Hydrogels for Regenerative Medicine Purposes. *Acta Biomater.* **2014**, *10*, 4787−4797.
(41) Cerqueira, M. T.; da Silva, L. P.; Santos, T. C.; Pirraco, R. P.; Correlo, V. M.; Marques, A. P.; Reis, R. L. Human Skin Cell Fractions Fail to Self-Organize within a Gellan Gum/Hyaluronic Acid Matrix but Positively Influence Early Wound Healing. *Tissue Eng., Part A* **2014**, *20*, 1369−1378.
(42) Wicke, C.; Halliday, B.; Allen, D.; Roche, N. S.; Scheuenstuhl, H.; Spencer, M. M.; Roberts, A. B.; Hunt, T. K. Effects of Steroids and Retinoids on Wound Healing. *Arch. Surg.* **2000**, *135*, 1265−1270.
(43) Liu, S.; Zhang, H.; Zhang, X.; Lu, W.; Huang, X.; Xie, H.; Zhou, J.; Wang, W.; Zhang, Y.; Liu, Y.; Deng, Z.; Jin, Y. Synergistic Angiogenesis Promoting Effects of Extracellular Matrix Scaffolds and Adipose-Derived Stem Cells During Wound Repair. *Tissue Eng., Part A* **2011**, *17*, 725−739.
(44) Auxenfans, C.; Lequeux, C.; Perrusel, E.; Mojallal, A.; Kinikoglu, B.; Damour, O. Adipose-Derived Stem Cells (Ascs) as a Source of Endothelial Cells in the Reconstruction of Endothelialized Skin Equivalents. *J. Tissue Eng. Regener. Med.* **2011**, *6*, 512−518.
(45) Bourin, P.; Bunnell, B. A.; Casteilla, L.; Dominici, M.; Katz, A. J.; March, K. L.; Redl, H.; Rubin, J. P.; Yoshimura, K.; Gimble, J. M. Stromal Cells from the Adipose Tissue-Derived Stromal Vascular Fraction and Culture Expanded Adipose Tissue-Derived Stromal/Stem Cells: A Joint Statement of the International Federation for Adipose Therapeutics and Science (Ifats) and the International Society for Cellular Therapy (Isct). *Cytotherapy* **2013**, *15*, 641−648.
(46) Fedorovich, N. E.; Oudshoorn, M. H.; van Geemen, D.; Hennink, W. E.; Alblas, J.; Dhert, W. J. The Effect of Photopolymerization on Stem Cells Embedded in Hydrogels. *Biomaterials* **2009**, *30*, 344−353.
(47) Ayala, R.; Zhang, C.; Yang, D.; Hwang, Y.; Aung, A.; Shroff, S. S.; Arce, F. T.; Lal, R.; Arya, G.; Varghese, S. Engineering the Cell-Material Interface for Controlling Stem Cell Adhesion, Migration, and Differentiation. *Biomaterials* **2011**, *32*, 3700−3711.
(48) Chen, Y. M.; Gong, J. P.; Tanaka, M.; Yasuda, K.; Yamamoto, S.; Shimomura, M.; Osada, Y. Tuning of Cell Proliferation on Tough Gels by Critical Charge Effect. *J. Biomed. Mater. Res., Part A* **2009**, *88*, 74−83.
(49) Schneider, G. B.; English, A.; Abraham, M.; Zaharias, R.; Stanford, C.; Keller, J. The Effect of Hydrogel Charge Density on Cell Attachment. *Biomaterials* **2004**, *25*, 3023−3028.
(50) Wang, C.; Gong, Y.; Lin, Y.; Shen, J.; Wang, D. A. A Novel Gellan Gel-Based Microcarrier for Anchorage-Dependent Cell Delivery. *Acta Biomater.* **2008**, *4*, 1226−1234.
(51) Klar, A. S.; Guven, S.; Biedermann, T.; Luginbuhl, J.; Bottcher-Haberzeth, S.; Meuli-Simmen, C.; Meuli, M.; Martin, I.; Scherberich, A.; Reichmann, E. Tissue-Engineered Dermo-Epidermal Skin Grafts Prevascularized with Adipose-Derived Cells. *Biomaterials* **2014**, *35*, 5065−5078.
(52) Montano, I.; Schiestl, C.; Schneider, J.; Pontiggia, L.; Luginbuhl, J.; Biedermann, T.; Bottcher-Haberzeth, S.; Braziulis, E.; Meuli, M.; Reichmann, E. Formation of Human Capillaries in Vitro: The Engineering of Prevascularized Matrices. *Tissue Eng., Part A* **2010**, *16*, 269−282.
(53) Chan, R. K.; Zamora, D. O.; Wrice, N. L.; Baer, D. G.; Renz, E. M.; Christy, R. J.; Natesan, S. Development of a Vascularized Skin Construct Using Adipose-Derived Stem Cells from Debrided Burned Skin. *Stem Cells Int.* **2012**, *2012*, 841203.
(54) Sun, G.; Shen, Y. I.; Kusuma, S.; Fox-Talbot, K.; Steenbergen, C. J.; Gerecht, S. Functional Neovascularization of Biodegradable Dextran Hydrogels with Multiple Angiogenic Growth Factors. *Biomaterials* **2011**, *32*, 95−106.
(55) Boyer, G.; Zahouani, H.; Le Bot, A.; Laquieze, L. In Vivo Characterization of Viscoelastic Properties of Human Skin Using Dynamic Micro-Indentation. *Conf. Proc. IEEE Eng. Med. Biol. Soc.* **2007**, *2007*, 4584−4587.
(56) Singer, A. J.; Clark, R. A. Cutaneous Wound Healing. *N. Engl. J. Med.* **1999**, *341*, 738−746.
(57) Metcalfe, A. D.; Ferguson, M. W. Tissue Engineering of Replacement Skin: The Crossroads of Biomaterials, Wound Healing, Embryonic Development, Stem Cells and Regeneration. *J. R. Soc., Interface* **2007**, *4*, 413−437.
(58) Slevin, M.; Kumar, S.; Gaffney, J. Angiogenic Oligosaccharides of Hyaluronan Induce Multiple Signaling Pathways Affecting Vascular Endothelial Cell Mitogenic and Wound Healing Responses. *J. Biol. Chem.* **2002**, *277*, 41046−41059.
(59) Tonello, C.; Zavan, B.; Cortivo, R.; Brun, P.; Panfilo, S.; Abatangelo, G. In Vitro Reconstruction of Human Dermal Equivalent Enriched with Endothelial Cells. *Biomaterials* **2003**, *24*, 1205−1211.
(60) Ibrahim, S.; Ramamurthi, A. Hyaluronic Acid Cues for Functional Endothelialization of Vascular Constructs. *J. Tissue Eng. Regener. Med.* **2008**, *2*, 22−32.
(61) Hendrickx, B.; Verdonck, K.; Van den Berge, S.; Dickens, S.; Eriksson, E.; Vranckx, J. J.; Luttun, A. Integration of Blood Outgrowth Endothelial Cells in Dermal Fibroblast Sheets Promotes Full Thickness Wound Healing. *Stem Cells* **2010**, *28*, 1165−1177.
(62) Crisan, M.; Yap, S.; Casteilla, L.; Chen, C. W.; Corselli, M.; Park, T. S.; Andriolo, G.; Sun, B.; Zheng, B.; Zhang, L.; Norotte, C.; Teng, P. N.; Traas, J.; Schugar, R.; Deasy, B. M.; Badylak, S.; Buhring, H. J.; Giacobino, J. P.; Lazzari, L.; Huard, J.; Peault, B. A Perivascular Origin for Mesenchymal Stem Cells in Multiple Human Organs. *Cell Stem Cell* **2008**, *3*, 301−313.
(63) da Silva Meirelles, L.; Caplan, A. I.; Nardi, N. B. In Search of the in Vivo Identity of Mesenchymal Stem Cells. *Stem Cells* **2008**, *26*, 2287−2299.

(64) Shepro, D.; Morel, N. M. Pericyte Physiology. *FASEB J.* **1993**, *7*, 1031−1038.
(65) Rehman, J.; Traktuev, D.; Li, J.; Merfeld-Clauss, S.; Temm-Grove, C. J.; Bovenkerk, J. E.; Pell, C. L.; Johnstone, B. H.; Considine, R. V.; March, K. L. Secretion of Angiogenic and Antiapoptotic Factors by Human Adipose Stromal Cells. *Circulation* **2004**, *109*, 1292−1298.
(66) Nie, C.; Yang, D.; Xu, J.; Si, Z.; Jin, X.; Zhang, J. Locally Administered Adipose-Derived Stem Cells Accelerate Wound Healing through Differentiation and Vasculogenesis. *Cell Transplant.* **2011**, *20*, 205−216.